

Proof by EPR Spectroscopy that the Unpaired Electron in an Os₂⁷⁺ Species Is in a δ* Metal-based Molecular Orbital

F. Albert Cotton,[§] Gina M. Chiarella,[†] Naresh S. Dalal,^{**†} Carlos A. Murillo,^{**†} Zhenxing Wang,[‡] and Mark D. Young[†]

[†]Department of Chemistry, P.O. Box 30012, Texas A&M University, College Station, Texas 77842-3012 and

[‡]Department of Chemistry, Dittmer Building, Florida State University, Tallahassee, Florida, 32306-4390

[§]Deceased February 20, 2007

Received October 21, 2009

Variable temperature structural and EPR studies are reported on the paddlewheel compound [Os₂(hpp)₄Cl₂]PF₆, **1**, (hpp = the anion of the bicyclic guanidine 1,3,4,6,7,8-hexahydro-2H-pyrimido[1,2-*a*]pyrimidine) that contains a rare M₂⁷⁺ species, with the goal of determining whether the unpaired electron resides in a metal- or ligand-based molecular orbital. Crystallographic studies show that the Os–Os distance in **1** remains essentially unchanged from 213 to 30 K, which is consistent with no changes in electronic structure in this range of temperature. It is noteworthy that the metal–metal distance in **1** is about 0.05 Å shorter than that in the precursor Os₂(hpp)₄Cl₂, which is consistent with the loss of an electron in a δ* orbital. EPR spectra of **1** were measured in dilute frozen solution, powder, and single crystals. The spectra were observable only below about 50 K, with an exceptionally large line width, ~3 750 gauss, for a powdered sample, due to dipolar interactions and to short relaxation times. There is a very small average *g* value of ~0.750 and a cylindrical symmetry about the Os–Os bond. These data are consistent with the unpaired electron orbital having a large *L* value, such as that of a δ* orbital. The combination of X-ray structural data, the short relaxation time, and the magnetic data provide strong evidence that the unpaired electron in this nine-electron Os₂⁷⁺ species is localized in a metal-based orbital with this electron residing predominantly in a δ* orbital rather than in a π* orbital and, thus, having an electronic configuration of σ²π⁴δ²δ*.

Introduction

Since the discovery of the first species with an unsupported quadruple bond having *D*_{4h} symmetry about four decades ago,¹ emphasis in the search for analogous compounds has provided a wealth of such species, most of which have bridging ligands and paddlewheel structures.² Common ligands employed to span the dimetal unit have been carboxylates and formamidates.² With very few exceptions, the M₂^{*n*+} cores in these compounds have formal charges, *n*, of 4, 5, and 6. Rare examples of compounds structurally characterized having lower oxidation numbers and tetragonal paddlewheel structures are those containing V₂³⁺ units³ as

well as a few compounds with trigonal paddlewheel structures having M₂³⁺ units, M = Fe⁴ and Co.⁵

More recently it has been found that bicyclic guanidinate ligands can stabilize dimetal units with unique characteristics.⁶ A notable example is that with M₂⁴⁺ units, M = Mo⁷ and W,⁸ spanned by four hpp ligands (hpp = the anion of 1,3,4,6,7,8-hexahydro-2H-pyrimido[1,2-*a*]pyrimidine). These guanidinate compounds have oxidation potentials at least 1.2 V lower than that of the formamidate or carboxylate analogues.⁹ In addition, the ionization potential for the ditungsten compound is so low that it is less than that of cesium,¹⁰ the textbook example of a stable element with the lowest known ionization energy.¹¹ The main reason for stabilization of the high oxidation states by these bicyclic

*To whom correspondence should be addressed. E-mail: dalal@fsu.edu (N.S.D.) and murillo@tamu.edu (C.A.M.).

(1) Cotton, F. A.; Curtis, N. F.; Harris, C. B.; Johnson, B. F. G.; Lippard, S. J.; Mague, J. T.; Robinson, W. R.; Wood, J. S. *Science* **1964**, *145*, 1305.

(2) *Multiple Bonds between Metal Atoms*; Cotton, F. A., Murillo, C. A., Walton, R. A., Eds.; Springer Science and Business Media, Inc.: New York, 2005.

(3) (a) Cotton, F. A.; Hillard, E. A.; Murillo, C. A. *J. Am. Chem. Soc.* **2003**, *125*, 2026. (b) Cotton, F. A.; Hillard, E. A.; Murillo, C. A.; Wang, X. *Inorg. Chem.* **2003**, *42*, 6063.

(4) (a) Cotton, F. A.; Daniels, L. M.; Falvello, L. R.; Matonic, J. H.; Murillo, C. A. *Inorg. Chim. Acta* **1997**, *256*, 269. (b) Cotton, F. A.; Feng, X.; Murillo, C. A. *Inorg. Chim. Acta* **1997**, *256*, 303.

(5) (a) Cotton, F. A.; Daniels, L. M.; Maloney, D. J.; Matonic, J. H.; Murillo, C. A. *Inorg. Chim. Acta* **1997**, *256*, 283. (b) Cotton, F. A.; Li, Z.; Murillo, C. A.; Poplaukhin, P. V.; Reibenspies, J. H. *J. Cluster Sci.* **2008**, *19*, 89.

(6) Coles, M. P. *Chem. Commun.* **2009**, 3659.

(7) (a) Cotton, F. A.; Durivage, J. C.; Gruhn, N. E.; Lichtenberger, D. L.; Murillo, C. A.; Van Dorn, L. O.; Wilkinson, C. C. *J. Chem. Phys. B* **2006**, *110*, 19793. (b) Cotton, F. A.; Murillo, C. A.; Wang, X.; Wilkinson, C. C. *Dalton Trans.* **2007**, 3943.

(8) Cotton, F. A.; Huang, P.; Murillo, C. A.; Wang, X. *Inorg. Chem. Commun.* **2003**, *6*, 121.

(9) Cotton, F. A.; Daniels, L. M.; Murillo, C. A.; Timmons, D. J.; Wilkinson, C. C. *J. Am. Chem. Soc.* **2002**, *124*, 9249.

(10) Cotton, F. A.; Gruhn, N. E.; Gu, J.; Huang, P.; Lichtenberger, D. L.; Murillo, C. A.; Van Dorn, L. O.; Wilkinson, C. C. *Science* **2002**, *298*, 1971.

(11) Cotton, F. A.; Wilkinson, G.; Murillo, C. A.; Bochmann, M. *Advanced Inorganic Chemistry*, 6th ed.; John Wiley & Sons, Inc.: New York, 1999.

ligands is the destabilization of the δ orbitals of the quadruply bonded unit because of a strong interaction with the $p\pi$ orbitals of the ligand.¹² It should be noted that guanidinate ligands can also stabilize to some extent high formal oxidation states in mononuclear compounds, and this type of ligand has become increasingly important in coordination chemistry.^{6,13}

Because of the ability of these bicyclic ligands to stabilize high oxidation numbers, exploration of the chemistry of paddlewheel complexes with such ligands has provided a series of compounds with M_2^{6+} cores.¹⁴ More importantly about six years ago, these ligands allowed the isolation of the first species with a formal M_2^{7+} core, $[\text{Os}_2(\text{hpp})_4\text{Cl}_2]\text{PF}_6$, **1**, for which two solvates, one having interstitial hexane and the other having acetone molecules, were structurally characterized, and the results were published in a preliminary communication.¹⁵ It should be noted that an important issue to be resolved when a dinuclear species is oxidized is whether the oxidation is metal- or ligand-based. It should be kept in mind that in general as the oxidation state of a dinuclear unit increases, the metal-based orbitals are expected to get smaller. This should diminish orbital overlap which may weaken metal–metal bond interactions. Additionally, with a strongly basic entity, such as the guanidinate ligands,¹⁶ there is a possibility that electron removal may take place at the ligand, not at the metal centers. Thus, for the oxidation of the diamagnetic species $\text{Os}_2(\text{hpp})_4\text{Cl}_2$ to $[\text{Os}_2(\text{hpp})_4\text{Cl}_2]\text{PF}_6$, it is essential to unambiguously determine whether an Os_2^{7+} core truly exists¹⁷ or if the process simply leads to oxidation of the guanidinate ligand. One of the few experimental techniques capable of differentiating between these two possibilities is EPR spectroscopy, since a ligand-based oxida-

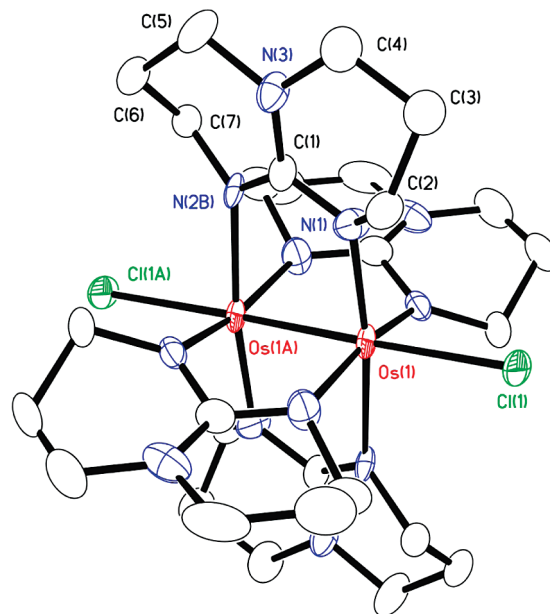


Figure 1. Structure of the cation in **1**·2acetone at 30 K with displacement parameters drawn at the 40% probability level. Hydrogen atoms have been omitted for clarity.

tion would be expected to yield an organic radical having a spectrum with a g value around the free-electron g value of 2.00, $g_e = 2.0023$.^{18,19} On the other hand, a metal-based oxidation in a species having transition-metal atoms would generally provide g values significantly different from g_e because of the interactions with the d orbitals.

Our early studies of **1**, carried out using powdered crystalline samples, provided EPR spectra having an extraordinarily broad signal with a line width of ~ 6000 G and a very low g of 0.791 ± 0.037 .¹⁵ Even though a g value so different from that of g_e is consistent with a metal-based molecular orbital, the lack of spectral resolution did not lead to definitive conclusions. One reason was that only powder samples were available for the EPR studies. Because the $[\text{Os}–\text{Os}]^{7+}$ species is a rare example of a high oxidation state, we have now carried out systematic studies using solutions, frozen glass, powder, and single crystals and provided conclusive evidence that indeed the unpaired electron resides in a metal-based δ^* molecular orbital, and the excessive line-widths can be attributed to dipolar interactions and fast spin–lattice relaxation.

Results and Discussion

Structural Considerations. Crystal structures for two solvates of **1** at 213 K have been described in detail elsewhere.¹⁵ In both **1**·2acetone and **1**·hexane, the $[\text{Os}_2(\text{hpp})_4\text{Cl}_2]^+$ cations are structurally very similar and have a paddlewheel structure, as shown in Figure 1 for **1**·2acetone at 30 K. The former crystallizes in the orthorhombic space group $Pnma$ ($Z = 4$) with dimetal units having idealized D_{4h} symmetry, while the latter has strict crystallographic D_{4h} symmetry since it crystallizes in the tetragonal space group $P4/mbm$ with $Z = 2$. As shown in Table 1, in both of these solvates the Os–Os distances are chemically indistinguishable at 213 K (2.3309(4) Å in **1**·2acetone and 2.3290(6) Å in **1**·hexane) and about 0.05 Å shorter than that in the precursor $\text{Os}_2(\text{hpp})_4\text{Cl}_2$

(12) Cotton, F. A.; Donahue, J. P.; Gruhn, N. E.; Lichtenberger, D. L.; Murillo, C. A.; Timmons, D. J.; Van Dorn, L. O.; Villagrán, D.; Wang, X. *Inorg. Chem.* **2006**, *45*, 201.

(13) See for example: (a) Foley, S. R.; Yap, G. P. A.; Richeson, D. S. *Polyhedron* **2002**, *21*, 619. (b) Soria, D. B.; Grundy, J.; Coles, M. P.; Hitchcock, P. B. *J. Organomet. Chem.* **2005**, *690*, 2315. (c) Coles, M. P.; Hitchcock, P. B. *Organometallics* **2003**, *22*, 5201. (d) Coles, M. P.; Hitchcock, P. B. *Dalton Trans.* **2001**, 1169. (e) Coles, M. P.; Hitchcock, P. B. *Inorg. Chim. Acta* **2004**, *357*, 4330. (f) Oakley, S. H.; Coles, M. P.; Hitchcock, P. B. *Inorg. Chem.* **2004**, *43*, 7564. (g) Coles, M. P.; Hitchcock, P. B. *Eur. J. Inorg. Chem.* **2004**, 2662. (h) Irwin, M. D.; Abdou, H. E.; Mohamed, A. A.; Fackler, J. P., Jr. *Chem. Commun.* **2003**, 2882. (i) Feil, F.; Harder, S. *Eur. J. Inorg. Chem.* **2005**, 4438. (j) Wilder, C. B.; Reifort, L. L.; Abboud, K. A.; McElwee-White, L. *Inorg. Chem.* **2006**, *45*, 263. (k) Rische, D.; Baunemann, A.; Winter, M.; Fischer, R. A. *Inorg. Chem.* **2006**, *45*, 269. (l) Edelmann, F. T. *Chem. Soc. Rev.* **2009**, 2253.

(14) Cotton, F. A.; Murillo, C. A.; Wang, X.; Wilkinson, C. C. *Inorg. Chim. Acta* **2003**, *351*, 191.

(15) Cotton, F. A.; Dalal, N. S.; Huang, P.; Murillo, C. A.; Stowe, A. C.; Wang, X. *Inorg. Chem.* **2003**, *42*, 670.

(16) (a) Novak, I.; Wei, X.; Chin, W. S. *J. Phys. Chem. A* **2001**, *105*, 1783. (b) Lee, T. H.; Rabalais, J. W.; J., W. *J. Electron Spectrosc. Relat. Phenom.* **1977**, *11*, 123.

(17) For a review of diosmium compounds, see: *Multiple Bonds between Metal Atoms*, Ren, T., Cotton, F. A., Murillo, C. A., Walton, R. A., Eds. Springer Science and Business Media, Inc.: New York, 2005, Chapter 10, p. 431.

(18) (a) For an example in tyrosyl radicals g values (g_x, g_y, g_z) range from 2.002 to 2.009. See: Un, S.; Gerez, C.; Elleingand, E.; Fontecave, M. *J. Am. Chem. Soc.* **2001**, *123*, 3048. (b) Similarly for the phenoxyl radical the spread of these values is 2.0022 to 2.0067. See: Benisvy, L.; Bittl, R.; Bothe, E.; Gamer, C. D.; McMaster, J.; Ross, S.; Teuloff, C.; Neese, F. *Angew. Chem., Int. Ed.* **2005**, *44*, 5314.

(19) For additional examples of systems of biological interest, see: (a) Kay, C. W.; Bittl, R.; Bacher, A.; Richter, G.; Weber, S. *J. Am. Chem. Soc.* **2005**, *127*, 10780. (b) Anderson, K. K.; Schmidt, P. P.; Katterle, B.; Stand, K. R.; Palmer, A. E.; Lee, S.-K.; Solomon, E. I.; Gräslund, A.; Barra, A.-L. *J. Biol. Inorg. Chem.* **2003**, *8*, 235. (c) Un, S.; Gerez, C.; Elleingand, E.; Fontecave, M. *J. Am. Chem. Soc.* **2001**, *123*, 3048.

Table 1. Comparison of the Core Distances (Å)

atoms	1·hexane at 213 K	1·2acetone at 213 K	1·2acetone at 30 K
Os–Os	2.3290(6)	2.3309(4)	2.3220(6)
Os–Cl	2.543(2)	2.520(1)	2.5034(17)
Os–N _{av}	2.045(7)	2.042(8)	2.039(8)

(Os–Os distance = 2.379(2) Å).²⁰ Furthermore, the metal–metal distance remains essentially constant (2.3220(6) Å as the temperature is lowered to 30 K (Tables 1 and 2). This is an indication that the electronic structure remains unchanged in the temperature range of 30–213 K, since changes in the electronic structure would be expected to show changes in the metal–metal distance, as has been demonstrated in a series of variable temperature structural and magnetic studies in diruthenium paddlewheel compounds.²¹

EPR Results. As shown in Figure 2a, the EPR spectrum of the powder of **1** at 6 K and at X-band (~9.4 GHz) is a broad signal centered at 9 080 G and an exceptionally large peak-to-peak width of 3 780 ± 50 G. The spectra become too weak to observe above about 50 K, in agreement with our preliminary data.¹⁵ The very low *g* value of 0.740, as compared to that of ~2.00 for organic radical cations,¹⁸ is consistent with the unpaired electron residing in an Os-based molecular orbital. This conclusion is additionally supported by the exceptionally large line width of ~3 775 G, as compared to that of at most 40–50 G expected for a carbon- or nitrogen-centered ligand-based radical.²²

To obtain further insight into the nature of this metal-based molecular orbital (MO), it was necessary to modify the experiment to reduce the line width of the EPR spectra. One significant cause of the large line width in solids is the dipolar coupling between the paramagnetic centers. Therefore, such couplings can generally be minimized by dilution of the sample in an appropriate solvent. When ~0.06 M solutions of **1** in CH₂Cl₂ were used, no signal was detectable above 175 K, indicating the spin–lattice relaxation time was very short. However, spectra were obtained upon freezing the solution to temperatures below 50 K, as shown in Figure 2b. The spectra consist of two clearly resolved peaks, labeled *g*_∥ and *g*_⊥, characteristic of a randomly oriented *S* = 1/2 paramagnetic compound with axial symmetry, without any hyperfine interaction. The assignment of *g*_∥ and *g*_⊥ (vide infra) has been made using what is customary for axial molecules with the peak labeled *g*_∥, arising from those molecules whose main symmetry axis is oriented along the applied field *H*, while that for *g*_⊥ corresponding to those oriented with their four-fold symmetry axes lying perpendicular to *H*. Figure 2c presents the simulation of the frozen glass EPR spectrum of Figure 2b, assuming *g*_x = *g*_y = *g*_⊥ and *g*_z = *g*_∥. The best-fit parameters are

*g*_∥ = 1.383 ± 0.004 and *g*_⊥ = 0.620 ± 0.002.²³ Since the Os–Os bond represents the main axis of symmetry in **1**, *g*_∥ corresponds to the Os–Os bond direction, and *g*_⊥ lies in the plane perpendicular to the direction of the Os–Os bond, as shown in the inset of Figure 2. In addition, the averaged *g* value [*g*_∥/3 + (2 × *g*_⊥)/3] of 0.874 is close to that of the powder spectra (0.740). It should be noted that the *g* anisotropy Δ*g* = 1.383 – 0.620 = 0.763 is significantly larger than that of mononuclear Os compounds²⁴ and other d⁵ species.²⁵

To determine the directions of the *g*_∥ and *g*_⊥ components relative to the molecular structure of **1**, single crystals were utilized. The crystals were rectangular plates, and X-ray studies established that the crystal plate corresponds to the 1 $\bar{1}$ 0 plane of the unit cell, as shown in Figure 3. The EPR spectra were obtained at 4.5 K by rotating the crystal at 10° intervals, as shown in Figure 4. From crystallographic data shown in Figure 3 and in the Supporting Information (Figure S3), it can be seen that the Os–Os bonds of the two magnetically independent molecules are oriented at approximately 8.835° from the *ab* plane (001), which means that the Os–Os bonds are nearly parallel to the *ab* plane. In general, the spectra should consist of two peaks for the two orientations of Os–Os bonds, but only one peak when the two peaks merge into one at an angle of about 100°, which only happens when the magnetic field is perpendicular to the *ab* plane (001) and is almost perpendicular to all of the Os–Os bonds. The measured *g* value using this approximation was 0.808,²⁶ which is close to *g*_⊥ = 0.620, indicating that *g*_⊥ corresponds to the perpendicular direction of Os–Os bond, and *g*_∥ lies along the Os–Os bond direction. This designation is in accordance with the idealized *D*_{4h} symmetry of **1** about the Os–Os bond and with the prediction of the simulations of the frozen glass spectra.

Implications on Electronic Structure. Magnetic data,²⁷ and to a lesser extent EPR data,²⁸ have been used to aid the determination of electronic structures of dimetal units. For **1**, the EPR data unambiguously support that the unpaired electron is in a metal-based orbital and, thus, verify that oxidation of Os₂(hpp)₄Cl₂ leads to an Os₂⁷⁺ unit. Because there are nine metal-based electrons in **1**, one of the electrons must be in an antibonding orbital,

(23) The simulation was done with Andrzej Ozarowski's program SPIN. For more information contact Dr. Andrzej Ozarowski at the National High Magnetic Field Laboratory in Tallahassee, Florida (ozarowsk@magnet.fsu.edu).

(24) See for example: (a) Ye, S.; Sarkar, B.; Duboc, C.; Fiedler, J.; Kaim, W. *Inorg. Chem.* **2005**, *44*, 2843. (b) Salmonsén, R. B.; Abelleira, A.; Clarke, M. J. *Inorg. Chem.* **1984**, *23*, 387. (c) Patra, S.; Sarkar, B.; Mobin, S. M.; Kaim, W.; Lahiri, G. K. *Inorg. Chem.* **2003**, *42*, 6469.

(25) However, it should be noted that there is a report of an EPR spectrum of *mer*-Os(PBu₂Ph)₃Cl₃ obtained on a single crystal at 100 K that has *g* = 3.30, 1.65, and 0.36. See: Rieger, P. H. *Coord. Chem. Rev.* **1994**, *135–136*, 203, and references therein.

(26) This method provides only an approximation because the Os–Os bonds are not aligned precisely with the crystallographic axis.

(27) See for example: (a) Miskowski, V.; Gray, H. B. *Top. Cur. Chem.* **1997**, *191*, 41. (b) Barral, M. C.; Jiménez-Aparicio, R.; Pérez-Quintanilla, D.; Priego, J. L.; Royer, E. C.; Torres, M. R.; Urbanos, F. A. *Inorg. Chem.* **2000**, *39*, 65. (c) Angaritis, P.; Cotton, F. A.; Murillo, C. A.; Villagrán, D.; Wang, X. *J. Am. Chem. Soc.* **2005**, *127*, 5008.

(28) (a) Telser, J.; Drago, R. S. *Inorg. Chem.* **1984**, *23*, 3114. (b) Drago, R. S.; Cosmano, R.; Telser, J. *Inorg. Chem.* **1984**, *23*, 3120. (c) Chen, W.-Z.; Cotton, F. A.; Dalal, N. S.; Murillo, C. A.; Ramsey, C. M.; Ren, T.; Wang, X. *J. Am. Chem. Soc.* **2005**, *127*, 12691.

(20) Clérac, R.; Cotton, F. A.; Daniels, L. M.; Donahue, J. P.; Murillo, C. A.; Timmons, D. J. *Inorg. Chem.* **2000**, *39*, 2581.

(21) (a) Cotton, F. A.; Murillo, C. A.; Reibenspies, J. H.; Villagrán, D.; Wang, X.; Wilkinson, C. C. *Inorg. Chem.* **2004**, *43*, 8373. (b) Chen, W.-Z.; Cotton, F. A.; Dalal, N. S.; Murillo, C. A.; Ramsey, C. M.; Ren, T.; Wang, X. *J. Am. Chem. Soc.* **2005**, *127*, 12691. (c) Cotton, F. A.; Herrero, S.; Jiménez-Aparicio, R.; Murillo, C. A.; Urbanos, F. A.; Villagrán, D.; Wang, X. *J. Am. Chem. Soc.* **2007**, *129*, 12666.

(22) Weil, J. Bolton, J. *Electron Paramagnetic Resonance: Elementary Theory and Practical Applications*, 2nd ed., Chapter 10; Wiley: New York, 2007.

Table 2. Selected Bond Distances (Å) and Angles (°) for **1**·2acetone at 30 K

atoms	bond length	atoms	bond length
Os(1)–Os(1A)	2.3220(6)	Os(1)–Cl(1)	2.5034(17)
Os(1)–N(1)	2.054(7)	Os(1)–N(2)	2.084(10)
Os(1)–N(4)	2.016(6)	Os(1)–N(5)	2.017(11)
atoms	bond angle (°)	atoms	bond angle (°)
N(1)–Os(1)–Cl(1)	91.12(16)	N(2)–Os(1)–Cl(1)	91.0(3)
N(4)–Os(1)–Cl(1)	91.65(18)	N(5)–Os(1)–Cl(1)	91.3(4)
N(1)–Os(1)–N(4)	90.1(3)	N(1)–Os(1)–N(5)	103.7(4)
N(2)–Os(1)–N(4)	78.8(4)	N(2)–Os(1)–N(5)	87.2(5)

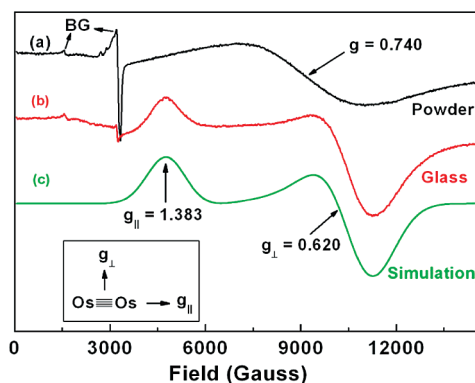


Figure 2. (a) EPR spectrum of the powder of **1** at 6 K and at X-band (~9.4 GHz). (b) X-band EPR spectrum of the frozen glass of **1**·2acetone at 15 K. (c) The simulation of the frozen glass EPR spectrum in (b). The inset shows the orientations of g components relative to the Os–Os bond. BG denotes background. See Supporting Information (Figures S1 and S2) for data showing the temperature dependence of the EPR spectra of powder samples.

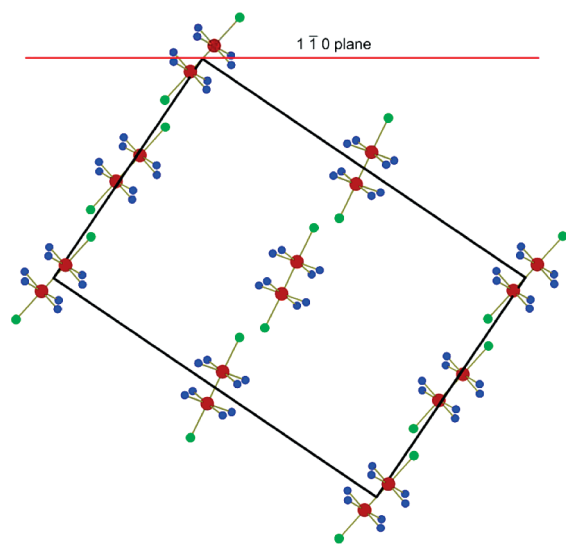


Figure 3. The orientation of the unit cell of **1**·2acetone relative to the crystal axes. The Os–Os bonds lie with an angle of 8.835° to the orthogonal plane. There are two magnetically distinct molecules in the unit cell. See also the Supporting Information, Figure S3.

and thus, the bond order in the dimetal unit is formally 3.5. However, there is some uncertainty as to whether the electronic configuration is either $\sigma^2\pi^4\delta^2\delta^*$ or $\sigma^2\pi^4\delta^2\pi^*$, since the relative energy of these orbitals may vary in some dimetal species, such as those containing Ru_2^{5+} units, which until recently has been commonly referred to as having an electronic configuration of the type

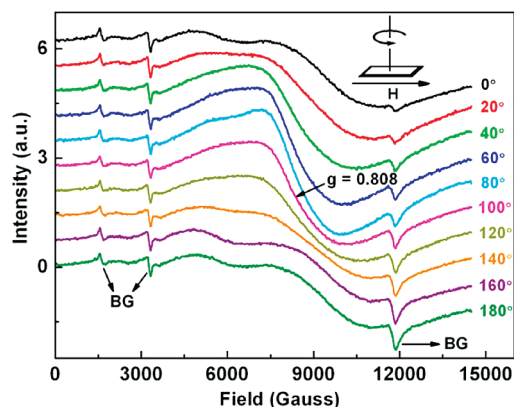


Figure 4. Angular dependence of the crystal of **1**·2acetone at 4.5 K. The inset shows how the plate-like crystal was rotated by keeping the magnetic field in the plane of the plate. Only a selected set of spectra are shown even though the measurements were done at 10° intervals. BG denotes background.

$\sigma^2\pi^4\delta^2(\delta^*\pi^*)^3$ because of the ambiguity of where the antibonding electrons are located.²⁹

For the diosmium system, it is known that the electronic configuration for the precursor of **1** is $\sigma^2\pi^4\delta^2\delta^*2$, since this molecule is diamagnetic.²⁰ Furthermore, removal of one electron from this precursor reduces the Os–Os distance by about 0.05 Å. This bond shortening is consistent with removal of an electron in an antibonding orbital. Furthermore, the magnitude of the decrease is in the range commonly observed when an electron from a δ orbital is removed from quadruple-bonded dimetal units, such as those having Mo_2^{4+} species.²⁹ These results strongly support the assignment of an electronic configuration of $\sigma^2\pi^4\delta^2\delta^*$ for **1**.

The EPR measurements help clarify this issue. The observed EPR line width of ~3 775 G cannot at all arise from an unpaired electron localized on an organic radical (either carbon- or nitrogen-centered) that is expected to be at most 40–50 G.²² Facts, such as the large line width and the signal is observable only below about 50 K, imply that the spin–lattice relaxation time, T_1 , of the Os_2^{7+} center is very short. An upper limit on the magnitude of T_1 can be obtained from the relationship $T_1 \approx \hbar/g\beta\Delta H$, where ΔH is the experimental line width.²² Using $\Delta H \approx 3 775$ G and $g = 0.740$, the value of $T_1 \approx 4 \times 10^{-11}$ s is obtained. Such a short excited-state lifetime, T_1 , strongly

(29) See for example: (a) Cotton, F. A.; Donahue, J. P.; Murillo, C. A.; Huang, P.; Villagrán, D. *Z. Anorg. Allg. Chem.* **2005**, *631*, 2606. (b) Cotton, F. A.; Hillard, E. A.; Murillo, C. A. *Inorg. Chem.* **2002**, *41*, 1639. (c) Cotton, F. A.; Dalal, N. S.; Liu, C. Y.; Murillo, C. A.; North, J. M.; Wang, X. *J. Am. Chem. Soc.* **2003**, *125*, 12945.

supports that the unpaired electron resides preferentially in a δ^* orbital rather than a π^* orbital.^{22,30}

It is important to note that these results are also in agreement with those in the only other M_2^{7+} species known, namely the Re_2^{7+} analogues that have been recently studied in our laboratories.³¹ These compounds also have a formal bond order of 3.5, but there is an important distinction in that the electronic configuration differs from that of **1** in the rhenium species, the configuration is the electron poor³² $\sigma^2\pi^4\delta$ that results from removal of an electron from a bonding δ orbital of the quadruply bonded precursor $Re_2(hpp)_4Cl_2$.³³

Conclusions

The present work has provided strong evidence that the compound $[Os_2(hpp)_4Cl_2]PF_6$, which contains an Os_2^{7+} core, has an unpaired electron in a metal-based orbital. Preliminary reports of an exceptionally low g value have been confirmed. Solution EPR studies have shown that the large line width observed in the powder spectra is a result of very large g anisotropy, dipolar interaction, and short relaxation time. A combination of structural and EPR techniques has shown that an electron is removed from the δ^* orbital upon oxidation from $Os_2(hpp)_4Cl_2$ to $[Os_2(hpp)_4Cl_2]^+$. The electronic configuration of this Os_2^{7+} species is $\sigma^2\pi^4\delta^2\delta^*$, and the formal bond order is 3.5. This work emphasizes the usefulness of EPR studies in the determination of electronic structures in metal-containing systems.

Experimental Section

Synthesis. The study focused on **1**·2acetone because it yielded crystals of better quality than **1**·hexane. Unless otherwise noted, all syntheses were carried out under an inert atmosphere using standard Schlenk techniques. Solvents were dried using a glass contour solvent system. Compound **1** was prepared using a slightly modified published procedure:¹⁵ to a flask charged with 0.200 g (0.200 mmol) of purple $Os_2(hpp)_4Cl_2$ and with 0.038 g (0.201 mmol) of $FcPF_6$ was added 20 mL of methylene chloride. After the mixture had been stirred for 30 min, the solvent was removed under vacuum. The residue was washed with ether (2×10 mL) and then extracted with acetone. This mixture was then filtered through a frit packed with Celite and the purplish-red solution layered with hexanes to produce very-dark crystals of **1**·2acetone. After filtration, crystals were handled in air.

EPR Studies. Low temperature (4–50 K) X-band (~4.8 GHz) EPR spectra were recorded on a Bruker E500 spectrometer using powdered, frozen glass, and single crystal samples. Single crystals enabled angular variation studies at 10° intervals with the magnetic field oriented in two mutually orthogonal crystal planes containing the Os–Os bonds. X-ray crystallography was used to relate the molecular orientation to the crystal morphology. Precise temperature control from 4 K up to ambient temperature was obtained by utilizing a continuous-flow liquid helium cryostat manufactured by Oxford Instru-

Table 3. Crystallographic Data for **1**·2acetone at 30 K

compound	1 ·2acetone
chemical formula	$[C_{28}H_{48}Cl_2N_{12}Os_2]PF_6 \cdot 2(C_3H_6O)$
fw	1265.21
cryst syst	orthorhombic
space group	<i>Pnma</i> (No. 62)
<i>a</i> (Å)	17.195(3)
<i>b</i> (Å)	25.155(5)
<i>c</i> (Å)	9.9897(18)
<i>V</i> (Å ³)	4321.1(13)
<i>Z</i>	4
d_{calc} , g·cm ⁻³	1.945
μ (mm ⁻¹)	6.110
2θ (°)	3.24–55.08
λ (Å)	0.71073
<i>T</i> (K)	30(2)
<i>R</i> ¹ ^a	0.0418
<i>wR</i> ² ^b (<i>I</i> > 2 σ (<i>I</i>))	0.1134

$$^a R1 = \sum ||F_o| - |F_c|| / \sum |F_o|, \quad ^b wR2 = [\sum [w(F_o^2 - F_c^2)^2] / \sum w(F_o^2)^2]^{1/2}, \\ w = 1/[\sigma^2(F_o^2) + (aP)^2 + bP], \quad \text{where } P = [\max(F_o^2 \text{ or } 0) + 2(F_c^2)]/3.$$

ments. The magnetic field was calibrated with a standard 2,2-diphenyl-1-picrylhydrazyl (DPPH radical with $g = 2.0037$) and a built-in NMR teslameter. The microwave frequency was monitored with a digital frequency counter. Powder samples were prepared by crushing crystalline material in high vacuum grease at room temperature. The frozen glass samples were prepared by dissolving the crystalline material in dichloromethane. Angle-dependence data were obtained using a single-axis goniometer attached to the sample tube.

Magnetization measurements were made using a quantum design SQUID magnetic property measurement system (MPMS XL) in a temperature range of 1.8–300 K and a field range of 0–7 T. The measurements agreed with earlier data¹⁵ and confirmed the presence of one unpaired electron ($S = 1/2$).

X-ray Structure Determination. Dark block-shaped purple crystals of **1**·2acetone were obtained in a week after adding a layer of 40 mL of isomeric hexanes to a 7 mL solution of the compound in acetone. A crystal measuring $0.20 \times 0.18 \times 0.15$ mm³ was coated with Paratone oil and mounted on a nylon Cryloop affixed to a goniometer head. The diffraction data were collected at 30 K using a Bruker SMART 1000 CCD area detector system equipped with an Oxford Helix cryostat. A full hemisphere of data was obtained by collecting 1271 frames using omega scans of 0.3° /frame with 20 s per frame. The first 50 frames were measured again at the end of the data collection to monitor for crystal decay, but no significant decomposition was observed. Cell parameters were determined using the program SMART.³⁴ Compound **1**·2acetone was uniquely identified as belonging to the orthorhombic space group *Pnma* by its systematic absences. Data reduction and integration were performed with the software package SAINT,³⁵ which corrects for Lorentz and polarization effects, while absorption corrections were applied by using the program SADABS.³⁶

The structure for **1**·2acetone was initially determined using the program XPREP from the SHELX software package.³⁷ The positions of the Os atoms were found via direct methods using the program SHELXTL.³⁸ Subsequent cycles of least-squares

(30) It should be noted that an unpaired electron in a π^* MO would involve substantial ligand character and, thus, would be expected to display less g anisotropy than that of an electron in an Os-based δ^* orbital.

(31) Cotton, F. A.; Dalal, N. S.; Huang, P.; Ibragimov, S. A.; Murillo, C. A.; Piccoli, P. M. B.; Ramsey, C. M.; Schultz, A. J.; Wang, X.; Zhao, Q. *Inorg. Chem.* **2007**, *46*, 1718.

(32) The term electron poor is used as defined in ref 2. For example, an M_2 species having a bond order of 3.5 and having 7 electrons has a $\sigma^2\pi^4\delta$ electronic configuration, while an electron-rich species with a similar 3.5 bond order has 9 electrons and has a $\sigma^2\pi^4\delta^2\delta^*$ electronic configuration.

(33) Cotton, F. A.; Gu, J.; Murillo, C. A.; Timmons, D. J. *J. Chem. Soc., Dalton Trans.* **1999**, 3741.

(34) SMART for Windows NT, version 5.618; Bruker Advanced X-ray Solutions, Inc.: Madison, WI, 2001.

(35) SAINT. Data Reduction Software, version 6.36A; Bruker Advanced X-ray Solutions, Inc.: Madison, WI, 2002.

(36) SADABS. Area Detector Absorption and other Corrections Software, version 2.03; Bruker Advanced X-ray Solutions, Inc.: Madison, WI, 2002.

(37) Sheldrick, G. M. SHELX-97 Programs for Crystal Structure Analysis, Institut für Anorganische Chemie der Universität: Göttingen, Germany, 1998.

(38) Sheldrick, G. M. SHELXTL, version 6.10; Bruker Advanced X-ray Solutions, Inc.: Madison, WI, 2000.

refinement followed by difference Fourier syntheses revealed the positions of the remaining non-hydrogen atoms. Hydrogen atoms were then added in idealized positions and included in the structure factor calculations. The asymmetric unit was comprised of a half of a paddlewheel cation and of an anion and half of two acetone molecules. During refinement it was noted that half of the nitrogen atoms in the hpp ligand and that all of the outer carbons adjacent to the nitrogen bound to the metal atoms were disordered. The disorder was successfully modeled using occupancies between 50.125 and 57.380% for the major components of the disordered units. Additional details of data collection at 30 K and of refinement for $\mathbf{1} \cdot 2$ acetone are provided in Table 3. Other crystallographic data are available as Supporting Information. All non-hydrogen atoms were refined with anisotropic displacement parameters. The core structure for $\mathbf{1} \cdot 2$ acetone is

presented in Figure 1. Selected bond distances and angles are listed in Table 2.

Acknowledgment. The work at Texas A&M University was supported by the Robert A. Welch Foundation and the Texas A&M University. C.A.M. also thanks the National Science Foundation (NSF) (IR/D support). The work at Florida State University was partially supported by NSF via grant no. NIRT-DMR 05-6946.

Supporting Information Available: X-ray crystallographic data for $\mathbf{1} \cdot 2$ acetone in standard CIF format. A figure showing the orientation of the Os–Os bond in $\mathbf{1} \cdot 2$ acetone as viewed along the *c*- and *a*-axes of the unit cell and figures showing the temperature dependence of the EPR spectra of powder samples. This material is available free of charge via the Internet at <http://pubs.acs.org>.